Hydration Process of Na_2^- in Small Water Clusters: Photoelectron Spectroscopy and Theoretical Study of $Na_2^-(H_2O)_n$†

Akimasa Fujihara, Chiyoko Miyata, Ayako Maekawa, and Kiyokazu Fuke*

Department of Chemistry, Kobe University, Nada, Kobe 657-8501, Japan

Kota Daigoku, Naomi Murata, and Kenro Hashimoto*

Department of Chemistry, Tokyo Metropolitan University, 1-1 Minami-Ohsawa, Hachioji-shi, Tokyo 192-0397, Japan

Received: January 29, 2007; In Final Form: April 24, 2007

Photoelectron spectroscopy (PES) of $Na_2^-(H_2O)_n$ ($n \leq 6$) was investigated to examine the solvation of sodium aggregates in small water clusters. The PES bands for the transitions from the anion to the neutral ground and first excited states derived from Na_2 ($1^1\Sigma_g^+$) and Na_2 ($1^3\Sigma_u^+$) shifted gradually to the blue, and those to the higher-excited states correlated to the $3^2S + 3^2P$ asymptote dropped down rapidly to the red and almost degenerated on the $1^3\Sigma_u^+$-type band at $n = 4$. Quantum chemical calculations for n up to 3 showed that the spectra can be ascribed to structures where one of the Na atoms is selectively hydrated. From the electron distributions, it is found that the $Na^- - Na^+(H_2O)_n^-$-type electronic state grows with increasing cluster size, which can be regarded as a sign of the solvation of Na_2^- with ionization of the hydrated Na.

1. Introduction

The structural and dynamical aspects of solvation process have been a central issue in solution chemistry for many years. Although many experimental and theoretical efforts have been made so far, the dynamics of solvation processes of electrons and metal ions in bulk solution is still a subject of intensive discussion.[1] To overcome this situation, gas-phase clusters with a limited number of solvent molecules have been investigated. They provide a model to gain the microscopic aspect of the solvation in the bulk.[2] Especially, the spectroscopic study on the solvated electrons and metal atoms/ions allows us to examine the stepwise changes in electronic structure of the solute molecules as functions of solvent number and type.[3,4] Photoabsorption and photoionization experiments of the solvated metal atoms/ions such as $M(NH_3)_n$ and $M(H_2O)_n$ (M = Li,[5,6] Na,[7,8] Cs,[9] Mg^+,[10,11] and Sr^+ [12,13]) have been carried out. For the Li and Na atoms, photoelectron spectroscopy of the negatively charged metal ions in the ammonia and water clusters has also been conducted to access the neutral ground and excited states of the solvated metal atoms.[6,14]

The ionization potentials,[15−21] electronic spectra,[22,23] and photoelectron spectra[24−27] of these clusters have also been examined theoretically to unveil what electronic states are behind the spectra. The quantum chemical studies have provided important information on not only the size but also the structure dependence of the electronic states. When the metal is surrounded by the solvents from N or O side, the electron transfer from the metal to the solvents proceeds with increasing n until around the size of the first-shell closure.[18,19,26,27] The spatial expansion of the unpaired electron occurs during this process, giving rise to a one-center ion-pair state.[26,27] For the metal−water clusters, it is found that the excess electron starts localization in a part of the surface of clusters by the further hydration in the second-shell, which can be regarded as the sign of the early stage of the formation of a two-center ion pair state.[19,22]

A unique system is the Na^- anion in the water clusters. From the analysis of the photoelectron spectra,[14,25] it has been known that the $Na^-(H_2O)_n$ complexes have the structure in which the water clusters are bound to the Na^- from H sides though the Na−O interaction is preferential in the neutral form.

Intimately related to the above issues, the dissolution of metal in a metal−liquid interface is also a fundamental process in various electrochemical systems. To construct a microscopic model of the dissolution process, where the formation of solvated electrons and/or metal ions induced by solute−solvent interaction is a key step, the solvent clusters containing Na aggregates are an interesting research target. The spectroscopic investigation of solvated Na aggregates allows us to answer how the solvent orientation enhances the electron transfer from solute to solvent and how many solvent molecules are required to dissolve the metal atom. In the previous work, we investigated the solvation process of Na aggregates in ammonia clusters by the photoelectron spectroscopy and ab initio calculations for the ammoniated Na aggregate anions.[28−30] We have also examined preliminary the photoelectron and photodissociation spectra of $Na_3^-(H_2O)_n$.[31]

In the present work, we studied the photoelectron spectroscopy (PES) of negatively charged Na_2 in water clusters to explore the solvation process of metal aggregate in small polar solvent clusters. The structures of $Na_2^-(H_2O)_n$ are particularly interesting because $Na^-(H_2O)_n$ have been found to form the clusters with the Na−H bonds contrary to the case of $Li^-(H_2O)_n$. The geometries, binding energies, and vertical detachment energies of these clusters are also calculated by using the *ab initio* molecular orbital (MO) method. On the basis of these

† Part of the "Roger E. Miller Memorial Issue".

* Corresponding authors. E-mail: K.F., fuke@kobe-u.ac.jp; K.H., hashimoto-kenro@c.metro-u.ac.jp.

10.1021/jp070756l CCC: $37.00
Published on Web 06/20/2007

results, we discuss the stepwise solvation of alkali-metal dimer - water clusters in relation to the ionization and dissociation of metal aggregates.

2. Methods

2.1. Experiment. The experimental apparatus used in the present work has been described elsewhere.[28] It consists of three differentially evacuated chambers; a negative ion source, a time-of-flight (TOF) mass spectrometer, and a magnetic-bottle type photoelectron spectrometer. Negatively charged sodium−water clusters are produced by a laser vaporization method coupled with a supersonic expansion. A mixture gas of He with water vapor at 273 K was expanded by a pulsed valve into a conical channel dug in an aluminum block. The third harmonic of a Nd:YAG laser (New Wave Research, Polaris II) was focused onto a sodium rod that was rotating and translating in the aluminum block. The metal atoms and clusters vaporized were entrained by the stream of the mixture gas in the channel and were expanded into the first differential vacuum chamber. The negative ions produced were introduced into the TOF mass spectrometer through a skimmer and accelerated to 800 eV by pulsed electric fields. For the photoelectron kinetic energy measurement, negative ions with a given mass-to-charge ratio were selected with a pulsed mass gate after flying 0.9 m. The cluster ions were decelerated and then irradiated with the fundamental, second, and third harmonics of a Nd:YAG laser (Quanta-Ray, GCR-12, typical laser fluence of ca. 5 mJ/cm^2). The detached electrons were analyzed by the magnetic bottle type photoelectron spectrometer. The electron signals were accumulated as a function of flight time in a digital storage oscilloscope.

To facilitate the assignment of the photoelectron spectra for $Na_2^-(H_2O)_n$, a population-labeling experiment was also conducted.[29] A depletion laser at 1907 nm (about 20 mJ/cm^2) was irradiated to the mass-selected ions 200 ns prior to the 1064-nm photodetachment laser to bleach an isomer with the detachment threshold of less than 0.65 eV. A first Stokes line of a YAG-laser fundamental (Spectra Physics, GCR-250) was used as the bleaching light source.

2.2. Theory. Geometries of $Na_2^-(H_2O)_n$ ($n = 0-3$) were optimized using the energy gradient technique at the MP2 level with the usual frozen core approximation. Vibrational analyses were carried out at each optimized structure to confirm the minima on the potential energy surfaces. The program used was GAUSSIAN03.[32] The binding energies, $\Delta E(n)$, were evaluated by the following formula:

$$-\Delta E(n) = E(Na_2^-(H_2O)_n) - E(Na^-) - E(Na) - nE(H_2O) \quad (1)$$

$\Delta E(n)$ is the total binding energy of the clusters from the isolated Na^- anion, Na atom, and n water molecules. The zero-point vibrational correction (ZPC) was included in $\Delta E(n)$ by using scaled harmonic frequencies. The scale factor, 0.956, was used as in the case of $Na(H_2O)_n$ clusters.[21] We have also corrected the basis set superposition error for the binding energies by the counterpoise correction (CPC).[33] The vertical detachment energies of $Na_2^-(H_2O)_n$ were calculated by the multireference single and double excitation configuration interaction (MRSDCI) method preceded by the complete active space self-consistent-field (CASSCF) calculations.[34−38] The active space for the CASSCF consisted of 10 molecular orbitals (MOs) corresponding to the 3s, 3p, and 4s orbitals of two Na atoms. For the singlet neutral, five states were averaged with equal weight, while for the triplet, four states were averaged. The natural orbitals obtained by the CASSCF method were used as one-particle functions in the MRSDCI calculation with the CASSCF references. All single and double excitations from the active orbitals and 2n occupied molecular orbitals corresponding to the lone pair electrons of water molecules were included in the MRSDCI. We used MOLPRO2002 for the MRSDCI calculation.[39] The 6-31++G(d,p) basis sets were used for all the calculations.

3. Results and Discussion

3.1. Mass Spectrum. A typical mass spectrum of the negative ions of sodium−water clusters is displayed in Figure 1. The $Na^-(H_2O)_n$ ions were observed with more abundant signal at $n = 4$. The cluster ions assignable to $NaO^-(H_2O)_n$ were also detected at the corresponding masses. Hydrated sodium hydroxide ions such as $NaOH^-(H_2O)_n$ were found to be minor species, which was dissimilar to the case of copper−water negative ions.[40] In addition to these cluster ions, the water clusters containing Na_2^- and Na_3^- were observed with significant intensities. For $Na_2^-(H_2O)_n$, a more intense signal was observed at $n = 3$. The enhanced stability of this cluster may be partly due to a sudden increase of the electron binding energy for $n = 3$ as mentioned later.

3.2. Photoelectron Spectra of $Na^-(H_2O)_n$. In the previous work,[14] we examined the photoelectron spectroscopy of $Na^-(H_2O)_n$ to study the effect of hydration on the geometric and electronic structures of Na atom in both anionic and neutral states. For later comparison, the PESs of $Na^-(H_2O)_n$ ($n = 0-7$) cited from ref 14 are shown in Figure 2. The spectra are recorded at the detachment energy of 4.66 eV (3.50 eV for $n \leq 1$). The spectra of $Na^-(H_2O)_n$ for n up to 7 all exhibit two bands as in the case of the other alkali-atom systems such as $Li^-(NH_3)_n$, $Na^-(NH_3)_n$, and $Li^-(H_2O)_n$, but the bands shift in the opposite direction. For the 1:1 complex, the 3^2S-type band shifts to the higher vertical detachment energy (VDE) by 0.21 eV with respect to the $Na(3^2S)-Na^-(^1S)$ transition at 0.55 eV. In the spectrum for $n = 2$, the former band is observed at the VDE of 0.99 eV, whereas the 3^2P-type band appears at 3.46 eV. Both bands gradually shift further to the higher VDE with increasing n. These shifts are in marked contrast to those of the metal-ammonia systems.[14] The amount of shifts for both the $3^2S-{}^1S$ and the $3^2P-{}^1S$ transitions is almost the same being as large as ca. 1.0 eV at $n = 7$ with respect to those for Na^-. The structures and binding energies of $Na^-(H_2O)_n$ for $n \leq 4$ have been calculated.[24,25] On the basis of the calculations, the observed photoelectron bands are ascribed to the transitions for the isomers with Na−H bonds. In this configuration, the electronic structure of the neutral alkali atoms is not affected appreciably by hydration because the 3s electron density is localized on the metal atom. Similar spectral shifts are usually observed for hydrated anions such as $X^-(H_2O)_n$ (X = Cu, F, Br, I).[41] Thus, the origin of the blue shift in VDE has been ascribed to much larger electrostatic interaction in the anionic state than that in the neutral state. The above features in the solvation of single alkali atom in clusters may be significantly altered in the Na_2−water cluster, because Na_2 is nonspherical and may have much larger polarizability than the metal atom itself.

3.3. Photoelectron Spectra of $Na_2^-(H_2O)_n$. Figure 3 shows the photoelectron spectra of $Na_2^-(H_2O)_n$ recorded at the detachment energy of 3.50 eV (355 nm). The PES of free Na_2^- has already been reported previously by Bowen and coworkers.[42] The first and second bands observed at 0.55 and 1.32 eV have been assigned to the transitions from the ground-state

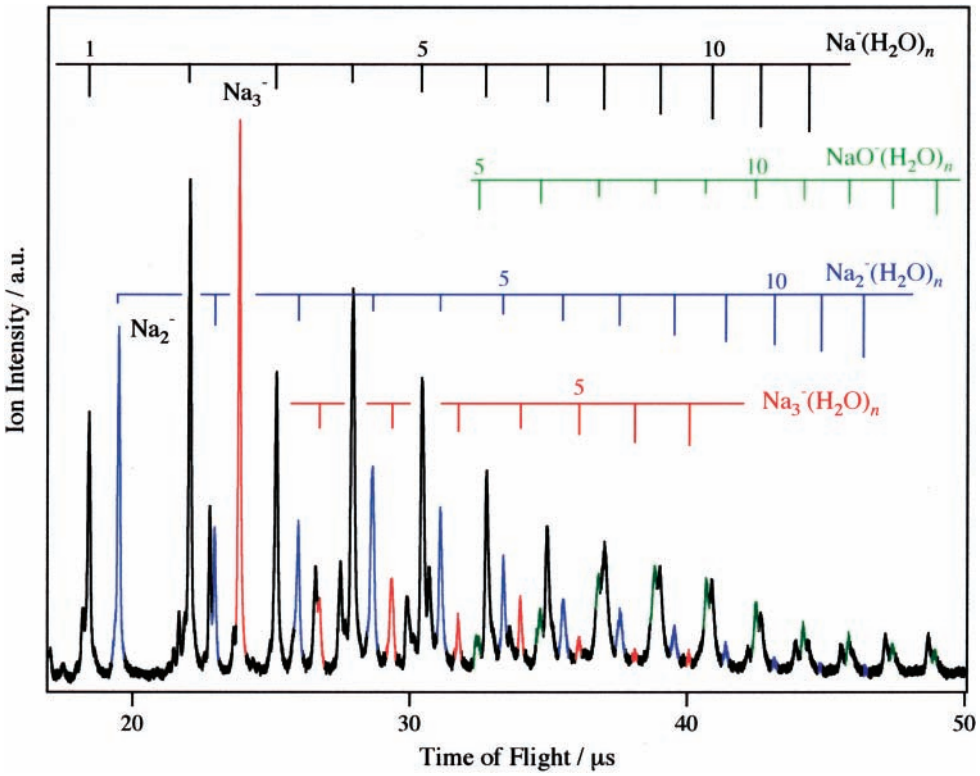

Figure 1. Typical mass spectrum of negatively charged Na−water clusters produced by the laser vaporization method coupled with supersonic expansion technique. The spectrum exhibits the formation of $Na^-(H_2O)_n$, $Na_2^-(H_2O)_n$, and $Na_3^-(H_2O)_n$. In addition to these clusters, $NaO^-(H_2O)_n$ ($n \geq 5$) are also detected in the higher mass region.

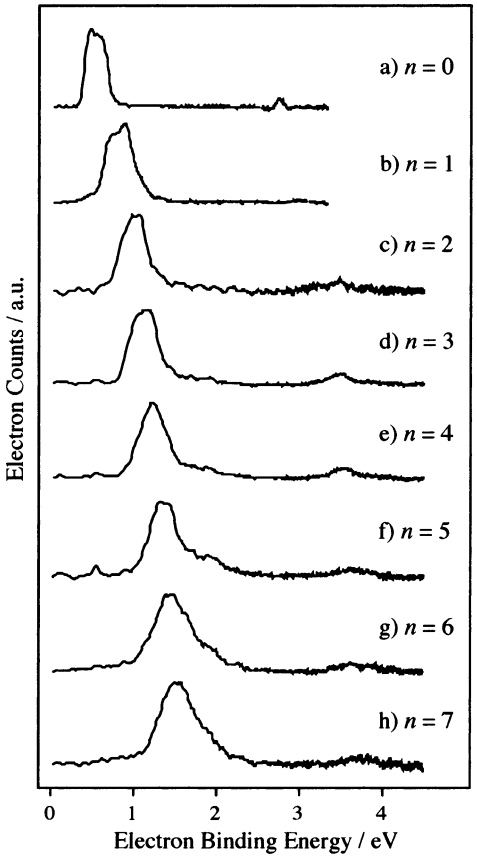

Figure 2. Photoelectron spectra of $Na^-(H_2O)_n$ cited from ref 14.

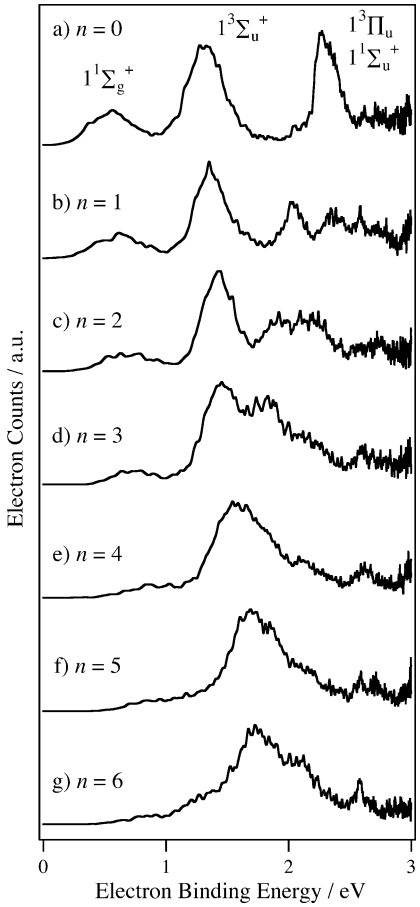

Figure 3. Photoelectron spectra of $Na_2^-(H_2O)_n$ recorded at the detachment energy of 3.50 eV (355 nm).

anion ($1^{-2}\Sigma_u^+$) to the neutral ground ($1^1\Sigma_g^+$) and first excited ($1^3\Sigma_u^+$) states correlated to the Na(3^2S) + Na(3^2S) asymptote, respectively. On the other hand, the third band at the 2.27-eV band has been ascribed to the transition to the $1^3\Pi_u$ and $1^1\Sigma_u^+$ states correlated to the Na(3^2S) + Na(3^2P) asymptote, which are accidentally degenerate in the anionic geometry. The VDEs

of the transitions to the $1^1\Sigma_g^+$, $1^3\Sigma_u^+$, $1^3\Pi_u$, and $1^1\Sigma_u^+$ states of Na_2 were 0.54, 1.21, 2.12, and 2.13 eV, respectively, by our MRSDCI calculations, which agreed well with those reported by Bonacic-Koutecky et al.[43] In our calculations, the VDEs for the higher excited states such as the $1^3\Sigma_g^+$, $2^1\Sigma_g^+$, and $1^1\Pi_u$ states were also predicted in the electron binding energy (EBE) range of 2.5−3.0 eV, but no PES band was observed in this region probably because of the low electron collection efficiency near the detachment energy.

For $Na_2^-H_2O$, four bands were observed at 0.57, 1.34, 2.03, and 2.35 eV in the energy region below 2.5 eV. The first band corresponds to the transition to the neutral ground state ($1^1\Sigma_g^+$) and exhibits a broad feature compared with that of bare Na_2^-. The second intense band derived from the $1^3\Sigma_u^+$ state shifted slightly to the higher EBE from $n = 0$. In contrast to the transitions to the states correlated to the Na(3^2S) + Na(3^2S) asymptote, those correlated to the Na(3^2S) + Na(3^2P) showed a quite different spectral change. The degenerate transitions ($1^3\Pi_u$ and $1^1\Sigma_u^+$) of Na_2^- at 2.27 eV were found to shift to 2.03 eV for $Na_2^-H_2O$. The origin of the 2.35-eV band is considered to be a new band derived from the further high state in Na_2, as will be described in detail in a later section.

The spectrum of $Na_2^-(H_2O)_2$ exhibited four bands at 0.6, 1.38, 1.90, and 2.16 eV, as shown in Figure 3c. With an addition of the second water molecule, the first two bands shifted to higher EBE, and the 2.03- and 2.35-eV bands of $n = 1$ shifted to the lower EBE by 0.13 and 0.19 eV, respectively. As seen in Figure 3d, VDEs of the neutral ground and first excited states in $Na_2^-(H_2O)_3$ shifted further to higher EBE compared with those for $n = 2$. Blue shifts were also observed for $n \geq 4$. The most drastic change in the PES was the extensive red shifts of the transitions derived from the states correlated to Na(^2S) + Na(^2P) as seen in Figure 3. The 1.90- and 2.16-eV bands of $Na_2^-(H_2O)_2$ further shifted down for $n \geq 3$ and merged into the transition to the first excited-state at 1.55 eV for $n = 4$.

To improve the resolution in the first-band region, we also measured the photoelectron spectrum with a detachment energy at 1.17 eV (1064 nm) and fitted the spectrum with Gaussian functions. The results are given in Figure 4. For Na_2^-, the transition to the neutral ground state, $1^1\Sigma_g^+ - 1^2\Sigma_u^+$, was observed at 0.55 eV. The PES of $Na_2^-H_2O$ exhibited a peak with a shoulder in the higher-energy region, as shown in Figure 4b. A curve fitting gave the VDEs of 0.48 and 0.78 eV. The $n = 2$ spectrum in Figure 4c may consist of at least three bands at 0.58, 0.74, and 0.87 eV, whereas the $n = 3$ spectrum in Figure 4d gave three bands peaked at 0.73, 0.81, and 0.88 eV. As shown in Figure 4e,f, we also observed similar PES bands for $n = 4$ and 5 as in the case of smaller clusters.

Figure 5 shows the spectrum recorded with a detachment energy at 2.33 eV (532 nm). The VDE of the $1^3\Sigma_u^+$ state for $n = 1$ was 1.36 eV. The band shifted to higher energy by 0.04 eV with respect to that of Na_2^-. The VDEs for the same transition for $n = 2$ and 3 were 1.38 and 1.44 eV, respectively. The spectra for $n = 4$ and 5 clearly exhibit that the higher-energy transitions merge into that to the first excited state at about 1.5 eV.

3.4. Optimized Structures and Energetics. Figure 6 shows the optimized structures and $\Delta E(n)$'s of $Na_2^-(H_2O)_n$ ($n \leq 3$). **Ia** is an *one-side* structure, in which a water molecule is bound to a single Na atom by an O atom. **Ib** is an *inserted* isomer, where the water molecule is inserted into two Na atoms. **Ic** and **Id** have *Na−H* forms with the water molecule bound to Na_2^- from the H-side. $\Delta E(1)$'s for **Ia** and **Ib** were 16.7 and 16.4 kcal/mol, respectively, which were greater than those of the *Na−H* clusters by more than 2 kcal/mol.

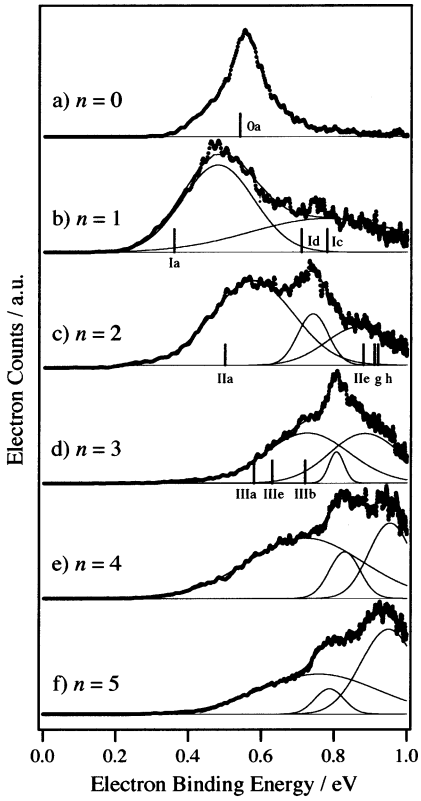

Figure 4. Photoelectron spectra of $Na_2^-(H_2O)_n$ recorded at the detachment energy of 1.17 eV (1064 nm). The spectra are fitted with Gaussian functions to reduce the peak positions of each band. The bars indicate the calculated VDEs of the isomers for each *n*.

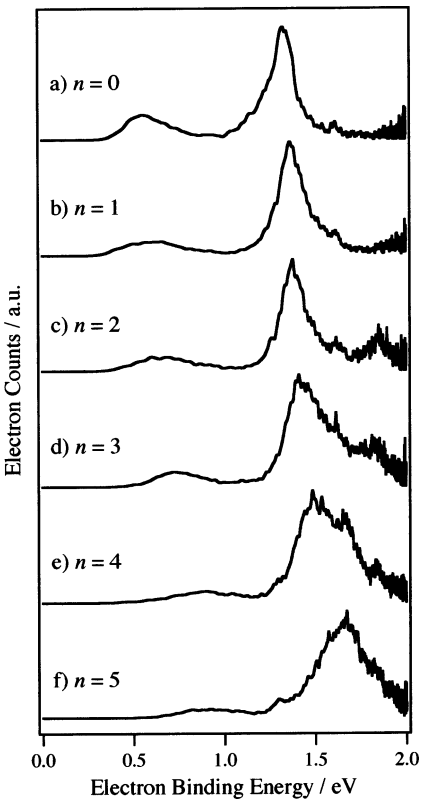

Figure 5. Photoelectron spectra of $Na_2^-(H_2O)_n$ recorded at the detachment energy of 2.33 eV (532 nm).

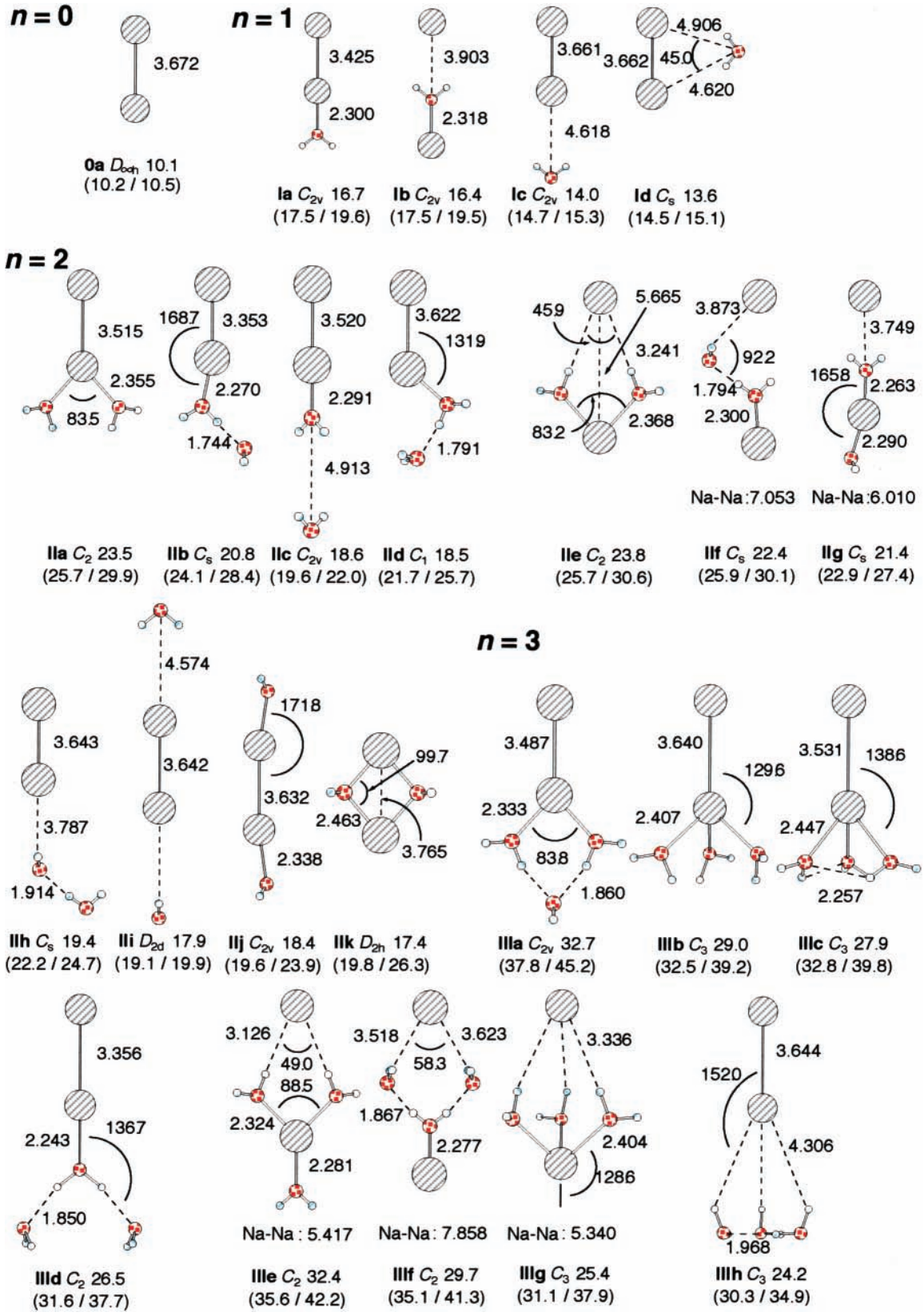

Figure 6. Optimized structures of $Na_2^-(H_2O)_n$ ($n = 0-3$) at the MP2/6-31++G(d,p) level. Geometric parameters are given in angstroms and degrees. Molecular symmetry and total binding energies, $\Delta E(n)$ (kcal/mol), with both ZP and CP corrections are given under each structure. The energies with only ZPC, and without those corrections, are also given in parentheses, respectively.

IIa-d, **IIe-g**, and **IIh-i** are the *one-side*, the *inserted* and the *Na−H* structures, respectively, for $n = 2$. The $\Delta E(2)$ values for **IIa** and **IIe** with two Na−O bonds were 23.5 and 23.8 kcal/mol, respectively. The other isomerswere less stable than those

structures by 1−6 kcal/mol. Though two more geometries, **IIj** and **IIk**, were optimized, they were much less stable than **IIa** and **IIe**.

For $n = 3$, the structures in which the third water molecule was bound to one of **IIa**, **IIb**, and **IIe-g**, were examined. **IIIa** and **IIIe** were the most stable. Their $\Delta E(3)$'s were 32.7 and 32.4 kcal/mol, respectively. The other $n = 3$ clusters were higher by more than about 3 kcal/mol.

It is interesting that the *inserted isomers*, **IIe** and **IIIe**, are as stable as the corresponding *one-side* complexes, **IIa** and **IIIa**, respectively. They can be regarded as an analog of each other in such a sense that Na_2 is asymmetrically solvated. As will be shown later, their electron distributions are also similar. The *inserted* clusters are the complexes between a bare Na^- and a hydrated Na atom whose stabilization energies are governed by the electrostatic interaction between the negative charge of free Na^- and the positive charges on the H atoms. On the other hand, one would expect an energy barrier for the formation of the **Ib** by breaking the Na−Na bond. The dissociation energy of the Na−Na^- bond amounted to 10.1 kcal/mol, as seen in $\Delta E(0)$.

3.5. Size and Structure Dependence of Vertical Detachment Energies and Contributors to Photoelectron Spectra. The calculated vertical detachment energies (cVDEs) of $Na_2^-(H_2O)_n$ ($n = 0-3$) are listed in Table 1. It is natural to expect that the transitions to the neutral ground state in the most stable structures are responsible for the spectra. The lowest-energy bands at 0.48 ($n = 1$), 0.58 ($n = 2$) and 0.73 ($n = 3$) eV in Figure 4, which are recorded by using the lowest detachment energy at 1.17 eV, can be assigned to the $1^1\Sigma_g^+$-type transition in the *one-side* structures. The cVDEs were 0.36, 0.50, and 0.58 eV in **Ia**, **IIa**, and **IIIa**, respectively, which agree with the experimental values within 0.13 eV. They decrease from **0a** to **Ia** and then increase from **Ia** to **IIIa** through **IIa**, being consistent with the observed band shifts.

In addition to these bands, other bands were observed in the higher-energy region for each *n*, as seen in Figure 4b−d. Their separations from the lowest band are 0.30 eV for $n = 1$, 0.16 and 0.29 eV for $n = 2$, and 0.08 and 0.15 eV for $n = 3$, respectively. The possible origins of those bands are the lowest-energy transitions of the other isomers or the higher vibrational transitions of the most stable forms. To examine these candidates, we carried out the population-labeling experiments,[29] in which the PES was recorded with an irradiation of the depletion laser (1907 nm) at 200 ns prior to the photodetachment laser. Figure 7 shows the PES of $Na_2^-H_2O$ with and without the depletion laser, respectively. It was found that the relative intensity of the first peak decreases appreciably by the irradiation of the depletion laser, indicating the bleaching of the most stable isomer by the laser irradiation. The rather weak depletion of the first band may be due to the overlapping of the bands at 0.65 eV, as expected from the fitted curves in Figure 4b. Thus these results suggest that two peaks in Figure 4b are ascribed not to the vibronic transitions, but to the lowest-energy transitions of the isomers.

Among the calculated local-minimum structures, the lowest cVDE of **Ib** did not match any band in Figures 3−5. This complex is considered to be scarcely formed in the molecular beam, probably due to the barrier mentioned before. For the other isomer **Ic** (**Id**), the cVDEs were 0.78(0.71) and 1.39(1.43) eV for the $1^1\Sigma_g^+$ and $1^3\Sigma_u^+$-type transitions, respectively. The former value agrees with the observed VDE at 0.78 eV, and the latter one may correspond to a weak tail observed at around 1.5 eV in Figure 5b. These isomers were less stable than **Ia** by 2.7−3.1 kcal/mol by the calculations. However, the above arguments, as well as the fact that the clusters are formed with nonequilibrium condition,[29] suggest the assignment of the observed band at 0.78 eV to the $1^1\Sigma_g^+$-type transition of these isomers with the Na−H bond. The cVDEs and the calculated binding energies for **Ic** and **Id** are very close to each other, and thus it is difficult to estimate their contributions to the observed band.

The population labeling experiments were also carried out for $Na_2^-(H_2O)_2$ using the Stokes line of the YAG fundamental at 1907 nm. However, no appreciable change in the relative spectral intensities was observed by the irradiation of the depletion laser in contrast to the case of $Na_2^-H_2O$. In the irradiation of the depletion laser, the isomer with the detachment energy smaller than the photon energy is bleached, and also it may be heated up through the absorption of the laser photons. In fact, we observed a strong absorption of the anion cluster in the energy region below the photodetachment threshold for $Na_3^-(H_2O)_3$.[31] These arguments would suggest that no spectral change in the above population labeling experiments is partly due to the redistribution of the isomers through an isomerization induced by the heating. Though the contribution of the isomers to the $n = 2$ PES is not clearly evidenced, no identification of the vibronic transition for $n = 1$ may rule out the assignment for the 0.74- and 0.87-eV bands to the vibrational origin, together with a few other reasons. At first, the harmonic bending frequency of the water in the neutral **IIa** was calculated to be ∼0.19 eV (1561 cm^{-1}), which was higher than the observed separation (0.16 eV). Second, the observed bands at around 0.8 eV for $n \geq 2$ are rather sharp, as shown in Figure 4. Similar sharp bands are also observed in the PESs of $Na_2^-(NH_3)_n$ recorded with the 1.17-eV detachment energy.[29] The PESs of these clusters were recently analyzed on the basis of the elaborated theoretical calculations.[44] It has been found that the lowest-energy transitions of the inserted isomers are a more plausible candidate for the higher bands than the vibrational transition.

From the comparison of the observed and calculated VDEs as well as the similarity of the spectral feature with $Na_2^-(NH_3)_n$, the 0.74-eV band was ascribed to the transition to the $1^1\Sigma_g^+$-type state in **IIe**, whose cVDE was 0.88 eV.

The PES of $Na_2^-(H_2O)_3$ also exhibits a sharp band at 0.81 eV as well as the rather broad one at 0.88 eV, as shown in Figure 4d.

The intense bands at 1.36 ($n = 1$), 1.38 ($n = 2$), and 1.44 ($n = 3$) eV in Figure 5 recorded by using the 2.33-eV detachment laser are ascribed to the $1^3\Sigma_u^+$-type transition in the *one-side* clusters, **Ia**, **IIa**, and **IIIa**, of which cVDEs were 1.28, 1.37, and 1.51 eV, respectively. The absolute values are close to the experimental ones, and their variations from Na_2^- to **IIIa** with increasing *n* reproduce well the band shifts, as in the case of the $1^1\Sigma_g^+$ -type transition. The same transition in **IIe**, whose cVDE was 1.34 eV, is expected to overlap on the 1.38-eV band for $n = 2$. The gradual increase of the bandwidth for the $1^3\Sigma_u^+$-type transitions for $n \geq 3$ is consistent with the growth of the inserted isomers with the similar binding energy for each *n*.

From the above arguments, the *one-side* isomers are expected to contribute to the spectral intensity in the energy region above 1.5 eV. The cVDEs for the $1^3\Pi_u$-type states were split by hydration and were 1.75 and 1.80 eV in **Ia**, which dropped off from that of Na_2^- by 0.37 and 0.32 eV, respectively, and cVDE for the $1^1\Sigma_u^+$-type transition was 1.97 eV, whose decrease from Na_2^- was 0.16 eV. From Na_2^- to **Ia**, the cVDEs for both the $1^3\Pi_u$- and $1^1\Sigma_u^+$-type transitions reduce, in agreement with the

TABLE 1: Vertical Detachment Energies (eV) in $Na_2^-(H_2O)_n$ Corresponding to Transitions from Anionic Ground State to Neutral Ground and Excited States at the MRSDCI Level

$n = 0$			$n = 1$									
	0a $D_{\infty h}$				**Ia** C_{2v}		**Ib** C_{2v}		**Ic** C_{2v}		**Id** C_s	
exp	sym	VDE	exp		sym	VDE	sym	VDE	sym	VDE	sym	VDE
0.55	$1\,^1\Sigma_g^+$	0.54	0.48	0.78	$1\,^1A_1$	0.36	$1\,^1A_1$	1.01	$1\,^1A_1$	0.78	$1\,^1A'$	0.71
1.32	$1\,^3\Sigma_u^+$	1.21	1.34		$1\,^3A_1$	1.28	$1\,^3A_1$	1.16	$1\,^3A_1$	1.39	$1\,^3A'$	1.43
2.27	$1\,^3\Pi_u$	2.12	2.03		$1\,^3B_1$	1.75	$1\,^3B_1$	2.55	$1\,^3B_1$	2.38	$2\,^3A'$	2.25
	$1\,^3\Pi_u$	2.12			$1\,^3B_2$	1.80	$1\,^3B_2$	2.70	$1\,^3B_2$	2.40	$1\,^3A''$	2.36
2.27	$1\,^1\Sigma_u^+$	2.13			$2\,^1A_1$	1.97	$2\,^1A_1$	1.88	$2\,^1A_1$	2.34	$2\,^1A'$	2.36
	$1\,^3\Sigma_g^+$	2.55	2.35		$2\,^3A_1$	2.20	$2\,^3A_1$	2.59	$2\,^3A_1$	2.76	$3\,^3A'$	2.81
	$2\,^1\Sigma_g^+$	2.87			$3\,^1A_1$	2.57	$3\,^1A_1$	3.00	$3\,^1A_1$	3.09	$3\,^1A'$	3.14
	$1\,^1\Pi_u$	2.95			$1\,^1B_1$	2.57	$1\,^1B_1$	2.61	$1\,^1B_1$	3.23	$4\,^1A'$	3.16
	$1\,^1\Pi_u$	2.95			$1\,^1B_2$	2.67	$1\,^1B_2$	2.72	$1\,^1B_2$	3.25	$1\,^1A''$	3.22

$n = 2$

			IIa C_2		**IIb** C_s		**IIc** C_{2v}		**IId** C_1		**IIe** C_2		**IIf** C_s		**IIg** C_s		**IIh** C_s		**IIi** D_{2d}		**IIj** C_{2v}		**IIk** D_{2h}	
exp			sym	VDE	sym	VDE	sym	VDE	sym	VDE	sym	VDE	sym	VDE	sym	VDE	sym	VDE	sym	VDE	sym	VDE	sym	VDE
0.58	0.74	0.87	$1\,^1A$	0.50	$1\,^1A'$	0.33	$1\,^1A_1$	0.60	$1\,^1A$	0.44	$1\,^1A$	0.88	$1\,^1A'$	1.21	$1\,^1A'$	0.91	$1\,^1A'$	0.92	$1\,^1A_1$	0.98	$1\,^1A_1$	0.35	$1\,^1A_g$	0.56
1.38			$1\,^3A$	1.37	$1\,^3A'$	1.33	$1\,^3A_1$	1.49	$1\,^3A$	1.15	$1\,^3A$	1.34	$1\,^3A'$	1.25	$1\,^3A'$	1.16	$1\,^3A'$	1.54	$1\,^3B_2$	1.59	$1\,^3A_1$	1.54	$1\,^3B_{2u}$	0.94
1.90			$1\,^3B$	1.78	$2\,^3A'$	1.70	$1\,^3B_2$	2.07	$2\,^3A$	1.85	$1\,^3B$	2.02	$2\,^3A'$	2.60	$3\,^3A'$	2.08	$1\,^3A''$	2.58	$1\,^3E$	2.66	$1\,^3B_2$	1.14	$1\,^3B_{3u}$	1.43
			$2\,^3B$	1.88	$1\,^3A''$	1.74	$1\,^3B_1$	2.02	$3\,^3A$	1.94	$2\,^3B$	2.34	$1\,^3A''$	2.73	$2\,^3A'$	2.11	$2\,^3A'$	2.59	$1\,^3E$	2.66	$1\,^3B_1$	1.46	$1\,^3B_{1u}$	1.62
			$2\,^1A$	1.80	$2\,^1A'$	2.03	$2\,^1A_1$	2.08	$2\,^1A$	1.86	$2\,^1A$	1.62	$2\,^1A'$	1.85	$2\,^1A'$	1.55	$2\,^1A'$	2.51	$1\,^1B_2$	2.54	$1\,^1B_2$	1.62	$2\,^1A_g$	1.97
2.16			$2\,^3A$	1.97	$3\,^3A'$	2.18	$2\,^3A_1$	2.33	$4\,^3A$	2.16	$2\,^3A$	2.20	$3\,^3A'$	2.74	$1\,^3A''$	2.22	$3\,^3A'$	2.93	$1\,^3A_1$	2.95	$2\,^3A_1$	1.79	$1\,^3A_g$	2.44
			$3\,^1A$	2.52	$3\,^1A'$	2.45	$3\,^1A_1$	2.70	$3\,^1A$	2.54	$3\,^1A$	2.81	$3\,^1A'$	2.72	$4\,^1A'$	2.55	$3\,^1A'$	3.23	$2\,^1A_1$	3.26	$2\,^1A_1$	2.08	$1\,^1B_{2u}$	1.99
			$1\,^1B$	2.35	$4\,^1A'$	2.50	$1\,^1B_2$	2.88	$4\,^1A$	2.59	$1\,^1B$	2.46	$1\,^1A''$	2.78	$3\,^1A'$	2.36	$1\,^1A''$	3.43	$1\,^1E$	3.51	$1\,^1B_1$	2.16	$1\,^1B_{3u}$	2.24
			$2\,^1B$	2.58	$1\,^1A''$	2.57	$1\,^1B_1$	2.77	$5\,^1A$	2.69	$2\,^1B$	2.68	$4\,^1A'$	3.17	$1\,^1A''$	2.32	$4\,^1A'$	3.45	$1\,^1E$	3.51	$3\,^1A_1$	2.28	$1\,^1B_{1u}$	2.36

$n = 3$

			IIIa C_{2v}		**IIIb** C_3		**IIIc** C_3		**IIId** C_2		**IIIe** C_2		**IIIf** C_2		**IIIg** C_3		**IIIh** C_3	
exp			sym	VDE	sym	VDE	sym	VDE	sym	VDE	sym	VDE	sym	VDE	sym	VDE	sym	VDE
0.73	0.81	0.88	$1\,^1A_1$	0.58	$1\,^1A$	0.72	$1\,^1A$	0.36	$1\,^1A$	0.53	$1\,^1A$	0.63	$1\,^1A$	1.47	$1\,^1A$	0.52	$1\,^1A$	0.92
1.44			$1\,^3A_1$	1.51	$1\,^3A$	1.37	$1\,^3A$	1.29	$1\,^3A$	1.52	$2\,^1A$	1.72	$1\,^3A$	1.50	$1\,^3A$	1.53	$1\,^3A$	1.55
1.81			$1\,^3B_1$	1.85	$1\,^3E$	1.93	$1\,^3E$	1.61	$1\,^3B$	1.88	$1\,^3A$	1.90	$1\,^3B$	2.79	$1\,^3E$	1.72	$1\,^3E$	2.56
			$1\,^3B_2$	1.88	$1\,^3E$	1.96	$1\,^3E$	1.64	$2\,^3B$	1.90	$1\,^3B$	2.13	$2\,^3B$	2.83	$1\,^3E$	1.74	$1\,^3E$	2.57
			$2\,^1A_1$	1.84	$2\,^1A$	1.58	$2\,^1A$	1.71	$2\,^1A$	2.13	$1\,^1B$	2.25	$2\,^1A$	1.78	$2\,^1A$	1.81	$2\,^1A$	2.52
2.02			$2\,^3A_1$	1.93	$2\,^3A$	1.98	$2\,^3A$	1.83	$2\,^3A$	2.19	$2\,^3A$	2.39	$2\,^3A$	2.80	$2\,^3A$	2.07	$2\,^3A$	2.96
			$3\,^1A_1$	2.46	$2\,^1A$	2.62	$2\,^1A$	2.37	$3\,^1A$	2.47	$3\,^1A$	2.47	$3\,^1A$	3.29	$2\,^1A$	2.61	$2\,^1A$	3.25
			$1\,^1B_1$	2.40	$1\,^1E$	2.36	$1\,^1E$	2.16	$1\,^1B$	2.68	$2\,^1B$	2.43	$1\,^1B$	2.94	$1\,^1E$	2.45	$1\,^1E$	3.43
			$1\,^1B_2$	2.52	$1\,^1E$	2.36	$1\,^1E$	2.17	$2\,^1B$	2.71	$2\,^3B$	2.48	$2\,^1B$	2.95	$1\,^1E$	2.47	$1\,^1E$	3.40

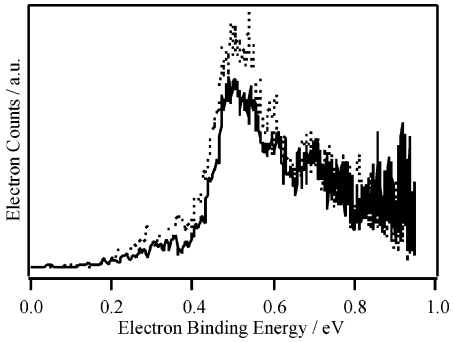

Figure 7. Photoelectron spectra of $Na_2^-H_2O$ with (solid line) and without (dotted line) the depletion laser at 0.65 eV. The decrease in the relative intensity of the 0.48-eV band was ascribed to the bleaching of the isomer **Ia**.

observed red shift of the 2.27-eV band for Na_2^-, but the change of the former seems large compared to the experimental value, 0.24 eV. Thus, the $1^1\Sigma_u^+$-type transition in **Ia** is considered to be the main contributor to the band peaked at 2.03 eV in Figure 3b, and the $1^3\Pi_u$-type transitions may overlap. The 2.35-eV band is probably due to the 2^3A_1 state in the neutral **Ia** derived from the $1^3\Sigma_g^+$ (Na_2). The cVDE was 2.20 eV, which agreed reasonably well with the band position and decreased from the corresponding value for the Na_2 by 0.35 eV.

The split $1^3\Pi_u$-type transitions in **IIa** were calculated at 1.78 and 1.88 eV, respectively, and the $1^1\Sigma_u^+$-type transition was at 1.80 eV. All the numbers correspond reasonably well to the 1.90-eV band in Figure 3c, though it is difficult to distinguish each transition in the spectrum. The broad 2.16-eV band is ascribed to the $1^3\Sigma_g^+$-type transition in **IIa**. The cVDE was 1.97 eV, being shifted down from the **Ia** by 0.23 eV. Both the absolute value and the decrease from $n = 1$ agree well with the observed spectrum, supporting the assignment. The calculations also predicted the $1^1\Sigma_u^+$-type transition in **IIe** at 1.62 eV, which may correspond to the small hump at 1.64 eV in Figure 5c. The transition in **IIe** is probably weak, as suggested by the intensity ratio of the isomer-band for the $1^1\Sigma_g^+$-type transition

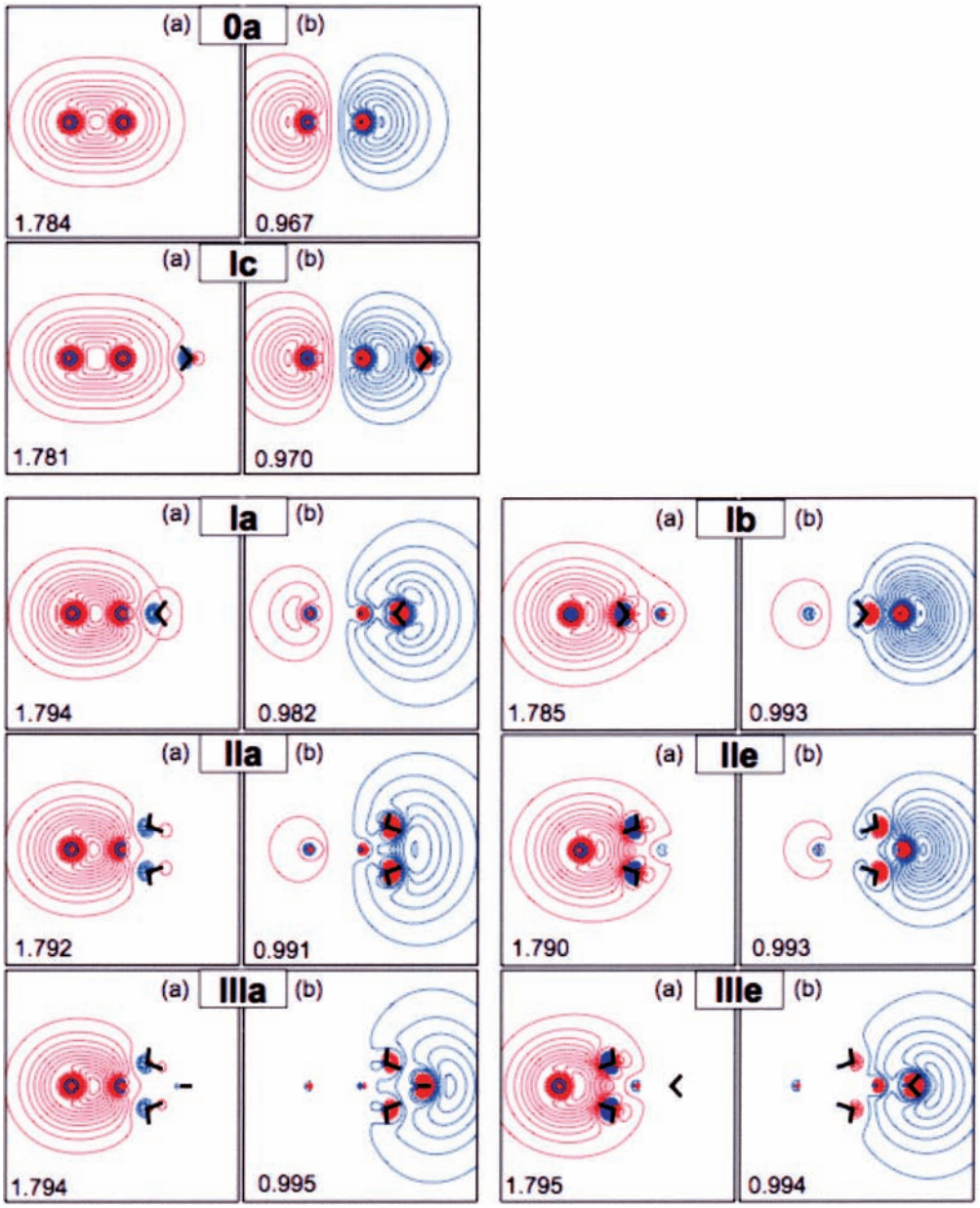

Figure 8. Contour maps of the NOs and their occupation numbers derived from the doubly occupied $4\sigma_g$ and singly occupied $4\sigma_u$ orbitals of Na_2^- for the MRSDCI wave functions in the ground state. The spacing of the contour is 0.005 $bohr^{-3/2}$, with red and blue lines for positive and negative values, respectively. The side length of each rectangle is 16 Å.

in Figure 4c, and is consistent with the observed spectrum. The cVDEs for the transition to the $1^3\Pi_u$- and $1^3\Sigma_g^+$-type states were 2.02−2.34 eV in **IIe**. They are slightly higher than the corresponding values in **IIa**, suggesting overlapping on the broad 2.16-eV band.

The cVDEs for the $1^3\Pi_u$-type transitions were 1.85 and 1.88 eV in **IIIa**, and that for the $1^1\Sigma_u^+$-type transition was 1.84 eV, in accordance with the 1.8-eV shoulder of the broad band at ∼1.5 eV in Figure 3d. The cVDE to the $1^3\Sigma_g^+$-type state was 1.93 eV, which reproduces well the 2.02-eV band. The slight decrease of the cVDE from **IIa** to **IIIa** is also consistent with the red shift of the band from 2.16 to 2.02 eV. As we have seen, the cVDEs for the transitions to the states correlated to the Na(3^2S) + Na(3^2P) asymptote decrease rapidly with increasing cluster size in the *one-side* structures. Indeed, the $1^3\Pi_u$ and $1^1\Sigma_u^+$ states were calculated to be above the $1^3\Sigma_u^+$ state by 0.91 eV in Na_2, but their separations were at most 0.37 eV in **IIIa**, in agreement with the coalescence of the corresponding PES bands at $n = 3$. On the other hand, the transitions to the $1^3\Sigma_u^+$- and $1^1\Sigma_u^+$-type states in **IIIe** were predicted at 1.90 and 1.72 eV, respectively, and those to the $1^3\Pi_u$-type and several other states were at energies higher than 2.0 eV. These results are compatible with the remarkable increase of the width of the 1.44-eV band from $n = 2$ to $n = 3$ and with the higher-energy tail above 2.0 eV in the $n = 3$ spectrum, which strongly supports the coexistence of the *one-side* and the *inserted* isomers in the molecular beam.

3.6. Hydration Process of Na_2 in Clusters. The above assignments for the first transitions of $Na_2^-(H_2O)_n$ ($n \leq 3$) indicate that the *one-side* isomers with Na−O bonds are the major contributor to the observed spectra. In addition, the transitions in the *inserted* isomers are merged in the spectra probably from $n = 2$, and the coexistence of the isomer bands is more likely from $n = 3$. Here, we describe the electronic change of Na_2^- induced by hydration in these clusters. The contour maps of the natural orbitals (NOs) for the MRSDCI wave functions of selected structures are shown in Figure 8. Those NOs are derived from the doubly occupied $4\sigma_g$ and singly occupied $4\sigma_u$ orbitals of Na_2^-. Both the $4\sigma_g$ and the $4\sigma_u$ orbitals are slightly deformed by the presence of water in the *Na−H* structure **Ic**. In contrast, the NOs are remarkably changed by the stepwise hydration in both the *one-side* (**Ia**, **IIa**, and **IIIa**) and the *inserted* (**Ib**, **IIe**, and **IIIe**) clusters. The $4\sigma_g$-type NOs tend to be pushed to the bare Na side, indicative of the formation of Na^-. On the other hand, the $4\sigma_u$-type NOs are distributed in the hydrated Na side being diffused with increasing cluster size. One can see that the $4\sigma_u$-type NO is squeezed out of the hydration shell in the $n = 3$ clusters, which is a sign of the ionization of the Na atom by hydration. In addition, the position of the large amplitude is located near the H atoms in the direction opposite to the free Na, indicating the {e^-}-H type interaction. The OH bonds play a role in trapping the excess electron near the cluster surface, which is similar to the case of $Li(H_2O)_n$ and $Na(H_2O)_n$ clusters.[21,23,24] Thus, the Na^-−Na^+-$(H_2O)_n^-$-type state grows in both the *one-side* and *inserted* clusters by hydration. A similar process has been examined in our previous works for $Na_3^-(NH_3)_n$ and $Na_3^-(H_2O)_n$.[29−31] To confirm the theoretical prediction for the dissociation process of negatively charged metal aggregates in small water clusters, we have also carried out the photodissociation experiments for $Na_3^-(H_2O)_3$.[31] A preferential formation of $Na_2^-(H_2O)_2$ suggesting the dissociation of Na_3 core in the anion state was observed. The above results as well as these indicate the dissociation of the Na_2^- core occurs in $Na_2^-(H_2O)_n$ by hydration, giving rise to the Na^- and hydrated Na^+.

4. Conclusion

We have examined the Na_2^- in water clusters by using the photoelectron spectroscopy and ab initio molecular orbital method for modeling the formation of solvated electrons and the dissolution of alkali metal in bulk solution. For $Na_2^-(H_2O)_n$ ($n \leq 3$), the water molecules are bound preferentially to one of the Na atoms by O atoms; Na_2 is asymmetrically solvated. We have also found that the VDEs of the transitions from the anion to the neutral ground and first excited states shift to the blue with respect to those of Na_2 ($1^1\Sigma_g^+$) and Na_2 ($1^3\Sigma_u^+$), in addition to the large red-shifting of the transitions to the higher excited states correlated to the Na(^{2}S) + Na(^{2}P) asymptote. The assignments of the observed spectra indicate that the *one-side* complexes are the major species for $n \geq 1$, and the *inserted* isomers are also considered to contribute to the spectra for $n \geq 2$. For these isomers, the Na^-−$Na^+(H_2O)_n^-$-type state grows by hydration, namely, the ionization of the Na_2^- core occurs by hydration, giving rise to the Na^- and hydrated Na^+.

Acknowledgment. This work is partially supported by the Grant-in-Aid for Scientific Research (Grants 16655008 and Grants 18350009) from the Ministry of Education, Culture, Sports, Science, and Technology (MEXT) of Japan, and also a research grant for the Japan Science and Technology Agency.

References and Notes

(1) Dogonadze, R. R., Kalman, E., Kornyshev, A. A., Ulstrup, J., Eds. *The Chemical Physics of Solvation*; Elsevier: Amsterdam, 1988; Part C.
(2) Castleman, A. W., Jr.; Keesee, R. G. *Chem. Rev.* **1986**, *86*, 589.
(3) Duncan, M. A. *Annu. Rev. Phys. Chem.* **1997**, *48*, 69.
(4) Fuke, K.; Hashimoto, K.; Iwata, S. In *Advances in Chemistry and Physics*; Prigogine, I., Rice, S. A., Eds.; John Wiley & Sons: New York, 1999; Vol. 100, Chapter 7, p.431.
(5) Takasu, R.; Hashimoto, K.; Fuke, K. *Chem. Phys. Lett.* **1996**, *258*, 94.
(6) Takasu, R.; Taguchi, T.; Hashimoto, K.; Fuke, K. *Chem. Phys. Lett.* **1998**, *290*, 481.
(7) Hertel, I. V.; Hüglin, C.; Nitsch, C.; Schulz, C. P. *Phys. Rev. Lett.* **1991**, *67*, 1767.
(8) Brockhaus, P.; Schulz, C. P.; Hertel, I. V. *J. Chem. Phys.* **1999**, *110*, 393.
(9) Misaizu, F.; Tsukamoto, K.; Sanekata, M.; Fuke, K. *Chem. Phys. Lett.* **1992**, *188*, 241.
(10) Yoshida, S.; Daigoku, K.; Okai, N.; Takahata, A.; Sabu, A.; Hashimoto, K.; Fuke, K. *J. Chem. Phys.* **2002**, *117*, 8657.
(11) Misaizu, F.; Sanekata, M.; Tsukamoto, K.; Fuke, K.; Iwata, S. *J. Phys. Chem.* **1992**, *96*, 8259.
(12) Shen, M. H.; Farrar, J. M. *J. Phys. Chem.* **1989**, *93*, 4386.
(13) Donnelly, S. G.; Farrar, J. M. *J. Chem. Phys.* **1993**, *98*, 5450.
(14) Takasu, R.; Misaizu, F.; Hashimoto, K.; Fuke, K. *J. Phys. Chem. A* **1997**, *101*, 3078.
(15) Barnett, R. N.; Landman, U. *Phys. Rev. Lett.* **1993**, *70*, 1775.
(16) Hashimoto, K.; He, S.; Morokuma, K. *Chem. Phys. Lett.* **1993**, *206*, 297.
(17) Hashimoto, K.; Morokuma, K. *J. Am. Chem. Soc.* **1994**, *116*, 11436.
(18) Hashimoto, K.; Morokuma, K. *J. Am. Chem. Soc.* **1995**, *117*, 4151.
(19) Hashimoto, K.; Kamimoto, T. *J. Am. Chem. Soc.* **1998**, *120*, 3560.
(20) Ramania, M.; Bernasconi, M.; Parrinello, M. *J. Chem. Phys.* **1998**, *109*, 6839.
(21) Tsurusawa, T.; Iwata, S. *J. Phys. Chem. A* **1999**, *103*, 6134.
(22) Schulz, C. P.; Bobbert, C.; Shimosato, T.; Daigoku, K.; Miura, N.; Hashimoto, K. *J. Chem. Phys.* **2003**, *119*, 11620.
(23) Bauschlicher, C. W., Jr.; Sodupe, M.; Partridge, H. *J. Chem. Phys.* **1992**, *96*, 4453.
(24) Hashimoto, K.; Kamimoto, T.; Fuke, K. *Chem. Phys. Lett.* **1997**, *266*, 7.
(25) Hashimoto, K.; Kamimoto, T.; Daigoku, K. *J. Phys. Chem. A* **2000**, *104*, 3299.
(26) Hashimoto, K.; Kamimoto, T.; Miura, N.; Okuda, R.; Daigoku, K. *J. Chem. Phys.* **2000**, *113*, 9540.

(27) Hashimoto, K.; Daigoku, K.; Kamimoto, T.; Shimosato, T. *Internet Electron. J. Mol. Des.* **2002**, *1*, 503. http://www.biochempress.com. ISSN 1538−6414, CODEN IEJMAT.

(28) Takasu, R.; Hashimoto, K.; Okuda, R.; Fuke, K. *J. Phys. Chem. A* **1999**, *103*, 349.

(29) Takasu, R.; Ito, H.; Nishikawa, K.; Hashimoto, K.; Okuda, R.; Fuke, K. *J. Electron. Sepctrosc. Relat. Phenom.* **2000**, *106*, 127.

(30) Fuke, K.; Hashimoto, H.; Takasu, R. In *Metal ion solvation and metal-ligand interactions*; Duncan, M. A., Ed.; Advances in metal and semiconductor clusters, Vol. 5; Elsevier: New York, 2001; p 1.

(31) Fujihara, A.; Miyata, C.; Fuke, K. *Chem. Phys. Lett.* **2005**, *411*, 345.

(32) Frisch, M. J.; Trucks, G. W.; Schlegel, H. B.; Scuseria, G. E.; Robb, M. A.; Cheeseman, J. R.; Montgomery, J. A., Jr.; Vreven, T.; Kudin, K. N.; Burant, J. C.; Millam, J. M.; Iyengar, S. S.; Tomasi, J.; Barone, V.; Mennucci, B.; Cossi, M.; Scalmani, G.; Rega, N.; Petersson, G. A.; Nakatsuji, H.; Hada, M.; Ehara, M.; Toyota, K.; Fukuda, R.; Hasegawa, J.; Ishida, M.; Nakajima, T.; Honda, Y.; Kitao, O.; Nakai, H.; Klene, M.; Li, X.; Knox, J. E.; Hratchian, H. P.; Cross, J. B.; Bakken, V.; Adamo, C.; Jaramillo, J.; Gomperts, R.; Stratmann, R. E.; Yazyev, O.; Austin, A. J.; Cammi, R.; Pomelli, C.; Ochterski, J. W.; Ayala, P. Y.; Morokuma, K.; Voth, G. A.; Salvador, P.; Dannenberg, J. J.; Zakrzewski, V. G.; Dapprich, S.; Daniels, A. D.; Strain, M. C.; Farkas, O.; Malick, D. K.; Rabuck, A. D.; Raghavachari, K.; Foresman, J. B.; Ortiz, J. V.; Cui, Q.; Baboul, A. G.; Clifford, S.; Cioslowski, J.; Stefanov, B. B.; Liu, G.; Liashenko, A.; Piskorz, P.; Komaromi, I.; Martin, R. L.; Fox, D. J.; Keith, T.; Al-Laham, M. A.; Peng, C. Y.; Nanayakkara, A.; Challacombe, M.; Gill, P. M. W.; Johnson, B.; Chen, W.; Wong, M. W.; Gonzalez, C.; Pople, J. A. *Gaussian 03*, revision c.02; Gaussian, Inc.: Wallingford, CT, 2004.

(33) Boys, S. F.; Bernardi, F. *Mol. Phys.* **1970**, *19*, 553.

(34) Werner, H. J.; Knowles, P. J. *J. Chem. Phys.* **1985**, *82*, 5053.

(35) Knowles, P. J.; Werner, H. J. *Chem. Phys. Lett.* **1985**, *115*, 259.

(36) Werner, H. J.; Knowles, P. J. *J. Chem. Phys*. **1988**, *89*, 5803.

(37) Knowles, P. J.; Werner, H. J. *Chem. Phys. Lett*. **1988**, *145*, 514.

(38) Knowles, P. J.; Werner, H. J. *Theor. Chim. Acta*. **1992**, *84*, 95.

(39) MOLPRO is a package of ab initio programs written by H.-J. Werner, and P. J. Knowles with contributions from R. D. Amos, A. Bernhardsson, A. Berning, et al.

(40) Misaizu, F.; Tsukamoto, K.; Sanekata, M.; Fuke, K. *Surf. Rev. Lett.* **1996**, *3*, 405.

(41) Robertson, W. H.; Johnson, M. A. *Ann. Rev. Phys. Chem.* **2003**, *54*, 173.

(42) McHugh, K. M.; Eaton, J. G.; Lee, G. H.; Sarkas, H. W.; Kidder, L. H.; Snodgrass, J. T.; Manaa, M. R.; Bowen, K. H. *J. Chem. Phys.* **1989**, *91*, 3792.

(43) Bonacic-Koutecky, V.; Fantucci, P.; Koutecky, J. *J. Chem. Phys.* **1990**, *93*, 3802.

(44) Hashimoto, K.; Shimizu, T.; Daigoku, K. *J. Phys. Chem. A* **2007**, *111*, 1990.